

Measured Instantaneous Viscous Boundary Layer in Turbulent Rayleigh-Bénard Convection

Quan Zhou^{1,2} and Ke-Qing Xia¹

¹*Department of Physics, The Chinese University of Hong Kong, Shatin, Hong Kong, China*

²*Shanghai Institute of Applied Mathematics and Mechanics, Shanghai University, Shanghai 200072, China*

(Dated: May 30, 2019)

We report measurements of the instantaneous viscous boundary layer (BL) thickness $\delta_v(t)$ in turbulent Rayleigh-Bénard convection. It is found that $\delta_v(t)$ obtained from the measured instantaneous two-dimensional velocity field exhibits intermittent fluctuations. For small values, $\delta_v(t)$ obeys a lognormal distribution, whereas for large values the distribution of $\delta_v(t)$ exhibits an exponential tail. The variation of $\delta_v(t)$ with time is found to be driven by the fluctuations of the large-scale mean flow velocity, as expected, and the local horizontal velocities close to the plate can be used as an instant measure of this variation. It is further found that the mean velocity profile measured in the laboratory frame can now be brought into coincidence with the theoretical Blasius laminar BL profile, if it is resampled relative to the time-dependent frame of $\delta_v(t)$.

PACS numbers: 44.25.+f, 44.20.+b, 47.27.-i

An important issue in the study of fluid dynamics is to determine the velocity within a very thin layer in the neighborhood of the plates and walls, i.e. viscous boundary layer (BL) [1]. The classical Prandtl-Blasius type BL, derived more than 100 years ago for flows over a flat plate, remains one of the few BLs with exact theoretical profile based on the equations of motion. For turbulent boundary layers, the well-known, empirical, logarithmic “law of wall” can be used to describe the shape of the velocity profile near the boundary. However, there are situations in which the BL is neither fully turbulent nor strictly laminar. How to characterize such BLs quantitatively has long been a challenge. An example is the turbulent Rayleigh-Bénard (RB) convection.

Despite many studies of the BL properties of the system [2, 3, 4, 5, 6, 7, 8, 9, 10], our understanding of the nature of the viscous BL in high-Rayleigh-number RB system remains incomplete. On the one hand, the time-averaged velocity field shares certain scaling properties with that of the Blasius-type laminar BL [10, 11]. On the other hand, the time-averaged velocity profile is found to differ from both the Blasius-type laminar BL and the turbulent logarithmic BL [9], especially for the region around the thermal BL where thermal plumes are generated. We note that, as the viscous BL is produced and stabilized by the viscous shear of the large-scale mean flow, the fluctuations of the large-scale velocity would cause the viscous BL to fluctuate as well, which would in turn cause a fixed measurement point to be sometimes inside and sometimes outside the BL [10]. In this respect, the time-averaged properties are not sufficient to reveal the dynamic nature of the BL. As fluctuating BLs exist in various flow systems, a more effective analysis method is thus highly desirable to unlock the intricate flow dynamics in the vicinity of plates, which is the objective of the present work.

This Letter reports measurements of the instantaneous viscous BL thickness $\delta_v(t)$ that shed new light on the nature of the BL. We use the RB convection as the test case

for the new representation method. The experiments cover the range $10^9 \lesssim \text{Ra} \lesssim 7 \times 10^{11}$ of the Rayleigh number $\text{Ra} = \alpha g \Delta H^3 / \nu \kappa$, with g being the gravitational acceleration, Δ temperature difference across the cell, H height of the cell, and α , ν , and κ being, respectively, the thermal expansion coefficient, kinematic viscosity, and thermal diffusivity of water. Two rectangular cells were used in the experiments and the details of which have been described elsewhere [12]. Briefly both cells are made of Plexiglas sidewall with upper and lower copper plates. The length, width, and height of the small cell are $25 \times 7 \times 24 \text{ cm}^3$ and those of the large cell are $81 \times 20 \times 76 \text{ cm}^3$. With this geometry, the large-scale flow is largely confined in the plane with the aspect ratio $\Gamma \simeq 1$ [12]. The coordinates are defined as follows: the origin coincides with the center of the bottom plate, the z -axis points upward and the x - and z -axes lie in the vertical circulation plane of the large-scale mean flow. During the measurements, both cells were levelled to within 0.1° and were filled with water at a mean temperature 40°C , corresponding to the Prandtl number $\text{Pr} = \nu / \kappa = 4.3$. The time-averaged statistical properties and various scaling behaviors of the viscous BL measured in the small cell have been reported previously [10]. Here we make new analysis to the data and present the results alongside with those from the new measurement in the large cell. For ease of reference, we give the experimental parameters for both cells.

The velocity fields close to the bottom plate were measured using the technique of particle image velocimetry (PIV). The details of the PIV measurements have been described previously [12], here we give only their main features. The seed particles for the large (small) cell experiments were $10\text{-}\mu\text{m}$ -diameter hollow glasses ($2.89\text{-}\mu\text{m}$ -diameter polyamid spheres) with density 1.03 (1.05) g/cm^3 . The measuring region had an area of 17.2×21.5 (11.1×13.8) mm^2 , corresponding to 63×79 velocity vectors, with a spatial resolution 0.27 (0.17) mm . The xz plane is chosen as the laser-illuminated plane, and hence

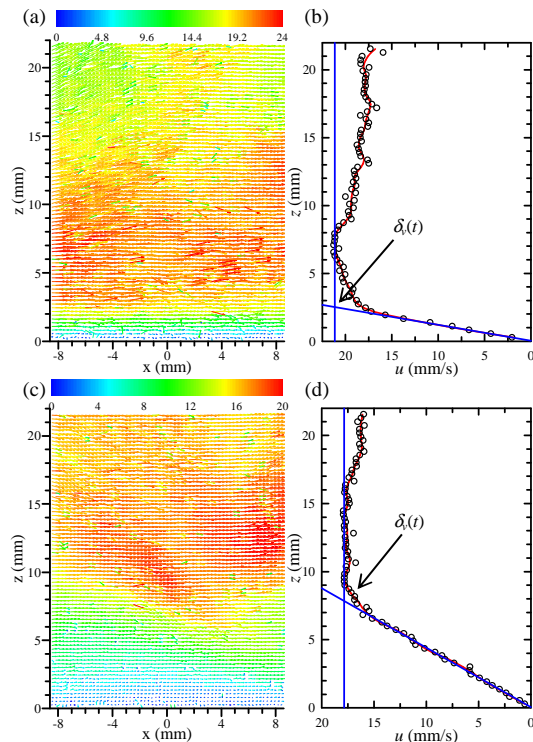


FIG. 1: (color online) (a) and (c) Two examples of the instantaneous velocity fields measured near the center of the bottom plate ($Ra = 1.9 \times 10^{11}$). (b) and (d) The horizontal velocity profiles $u(z, t)$ corresponding to those in (a) and (c), but averaged over $-2 \text{ mm} \leq x \leq 2 \text{ mm}$. The magnitude of the velocity in (a, c) is coded in both color scale and the length of the arrows in unit of mm/s. The solid lines in (b, d) illustrate how $\delta_v(t)$ is obtained.

the horizontal velocity component $u(x, z, t)$ and the vertical one $w(x, z, t)$ were measured. The large (small) cell measurement for each Ra lasted 4.42 (3.79) hours in which a total of 35000 (30000) vector maps were acquired at a sampling rate ~ 2.2 Hz.

Figures 1(a) and 1(c) show two examples of the instantaneous velocity fields. It is seen that the velocity fields near the plate show strong fluctuations and larger velocity magnitude yields thinner viscous BL. To obtain more quantitative information, we calculate this fluctuating BL thickness from the instantaneous velocity field using the following procedure. To reduce data scatter, we first coarse grain the measured velocity field by averaging it along the x -direction over a range of 2 mm for the small cell and 4 mm for the large cell. This yields the horizontal velocity profile $u(x, z, t)$ at time t . As the profile shows only weak x -dependence, we will hereafter present and discuss results measured at the center of the plate, i.e. $u(z, t) \equiv u(0, z, t)$ [circles in Figs. 1(b) and 1(d)]. Next, to increase the statistical accuracy, each profile is smoothed by using the locally weighted scatterplot smoothing method [13] [solid curves in Figs. 1(b) and 1(d)]. A linear fitting is then made to the smoothed profile $u_s(z, t)$ close to the plate. Denote the maximum

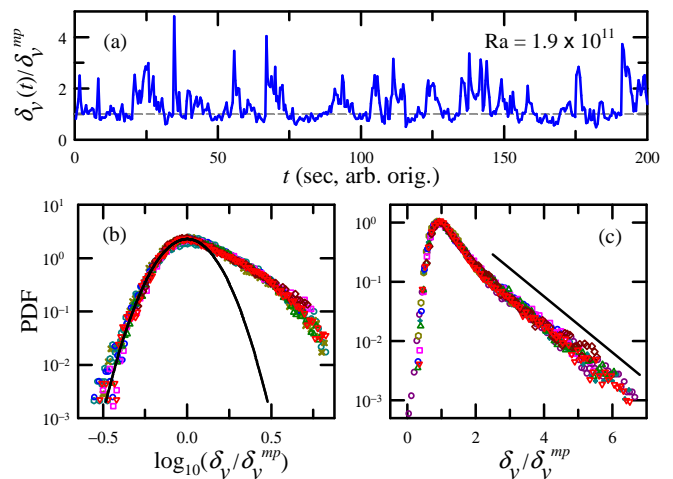


FIG. 2: (color online) (a) A sample time trace of instantaneous viscous BL thickness $\delta_v(t)$, normalized by its most-probable value δ_v^{mp} . (b) PDFs of $\log_{10}(\delta_v/\delta_v^{mp})$ and (c) those of δ_v/δ_v^{mp} measured at various Ra varying from 1.25×10^9 to 6.4×10^{11} . The solid curve in (b) marks the lognormal distribution for reference.

velocity of $u_s(z, t)$ as $u_m(t)$, the instantaneous viscous BL thickness $\delta_v(t)$ is then obtained as the distance from the plate at which the extrapolation of the linear fitting of $u_s(z, t)$ crosses $u_m(t)$. The uncertainty of $\delta_v(t)$, primarily due to uncertainties of $u_m(t)$ and the linear fitting to $u_s(z, t)$ close to the plate, is estimated to be about 3%. We note that the results are robust and insensitive to the algorithm used to smooth the profile.

Figure 2 shows a 200-second time trace of $\delta_v(t)$, normalized by the most-probable thickness δ_v^{mp} . One sees that the fluctuating $\delta_v(t)$ exhibits intermittent features, i.e., the amplitude of $\delta_v(t)$ can be much larger than its mean or most-probable value. We find that, for all measured values of Ra , δ_v^{mp} coincides with the viscous BL thickness λ_v (to within 4%) [10], defined through the slope of the time-averaged velocity profile at the plates that have been previously studied extensively. The probability density functions (PDF) of $\log_{10}(\delta_v/\delta_v^{mp})$ and δ_v/δ_v^{mp} are plotted in Figs. 2(b) and 2(c) respectively. For either PDF there is reasonable collapse for all measured Ra from both cells, which suggests a universality of the BL dynamics in turbulent RB system. In addition, it is seen that the tails of the PDFs at large δ_v ($> \delta_v^{mp}$) can be described by a decaying exponential distribution, whereas those at small δ_v ($\lesssim \delta_v^{mp}$) satisfy a lognormal statistics. The mechanism that leads to the different distributions of δ_v below and above its most probable values is at present unknown and would be a challenge for future theoretical studies.

The relation between $\delta_v(t)$ and the large-scale mean wind can be revealed by the cross-correlation function $g_m(\tau) = \langle \delta_v(t)u_m(t-\tau) \rangle / \sqrt{\langle \delta_v(t)^2 \rangle \langle u_m(t)^2 \rangle}$, where $\langle \dots \rangle$ denotes a time average. Figure 3(a) shows $g_m(\tau)$ as a function of time lag τ . Two features are worthy of note.

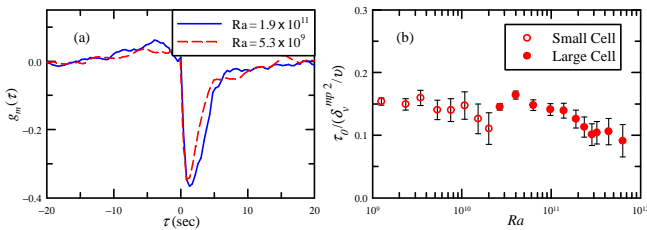


FIG. 3: (color online) (a) Cross-correlation function $g_m(\tau)$ between $\delta_v(t)$ and $u_m(t)$. (b) The normalized peak position τ_0 of $g_m(\tau)$ as a function of Ra.

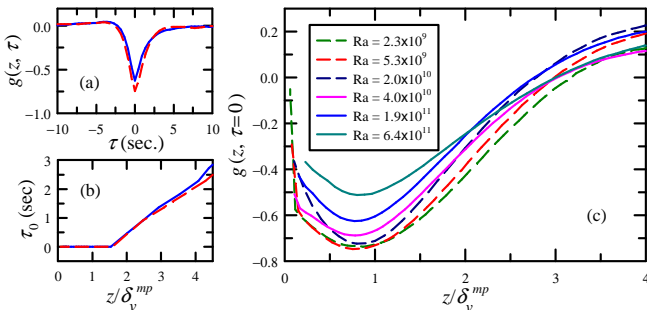


FIG. 4: (color online) (a) Cross-correlation function $g(z, \tau)$ between $\delta_v(t)$ and $u(z, t)$ measured at $z = 0.76\delta_v^{mp}$ and (b) the measured peak position τ_0 as a function of z/δ_v^{mp} . In both (a) and (b), dashed line: $Ra = 5.3 \times 10^9$ and solid line: 1.9×10^{11} . (c) The correlation coefficient $g(z, \tau = 0)$ as a function of z for several values of Ra.

(i) There exists a strong negative correlation between δ_v and u_m , which implies that the larger u_m is, the smaller δ_v becomes. (ii) The negative peak of $g_m(\tau)$ is located at a positive time lag τ_0 , indicating that the fluctuations of u_m leads the variation of δ_v . This is because a time delay is needed to transfer the momentum from the mean wind to the interior of the BL. Figure 3(b) shows the Ra-dependence of τ_0 , normalized by the typical timescale δ_v^{mp2}/ν of momentum transfer across the BL via viscosity. It is seen that $\tau_0/(\delta_v^{mp2}/\nu)$ varies around 0.14 for $Ra \lesssim 10^{11}$ and decreases slightly with increasing Ra for $Ra \gtrsim 10^{11}$. Here, the decrease of $\tau_0/(\delta_v^{mp2}/\nu)$ at high Rayleigh numbers suggests an increased contribution from Reynolds stress to the total shear stress inside the BL [10]. Direct study of shear stress around the viscous BL further reveal that Reynolds stress becomes more important than viscous stress for $Ra \gtrsim 10^{11}$ [10] and hence the BL would experience a transition from being laminar to a turbulent one.

We next examine the relation between $\delta_v(t)$ and the horizontal velocities close to the plate. We calculate the cross-correlation function between $\delta_v(t)$ and $u(z, t)$, i.e. $g(z, \tau) = \langle \delta_v(t)u(z, t - \tau) \rangle / \sqrt{\langle \delta_v(t)^2 \rangle \langle u(z, t)^2 \rangle}$, for each measuring vertical position z and for each Ra. Figure 4(a) shows two examples $g(z, \tau)$ measured inside the viscous BL. A strong negative peak can also be seen for both correlations, and the fact that the peaks are located at

$\tau_0 = 0$ suggests that the thinning of the viscous BL and the increasing of $u(z, t)$ occur simultaneously. We further note that $\tau_0 = 0$ holds for $z \lesssim 1.5\delta_v^{mp}$ for all Ra [see, e.g., Fig. 4(b)] and hence it is a BL property. For larger z a positive τ_0 is obtained, again indicating that the variation of $\delta_v(t)$ is driven by the large-scale mean wind. Figure 4(c) shows the correlation coefficient $g(z, \tau = 0)$ vs. z/δ_v^{mp} . One sees that $\delta_v(t)$ and $u(z, t)$ are highly correlated inside and around the viscous BL for all Ra. This suggests that the fluctuations of horizontal velocity measured locally close to the plate (e.g. at a single point) can be used as an instantaneous measure of the fluctuations of the viscous BL thickness $\delta_v(t)$, whereas the measurement of $\delta_v(t)$ itself would require measuring the entire velocity profile.

With the measured $\delta_v(t)$, we can now study the velocity profile in the reference frame of $\delta_v(t)$. We define the time-dependent relative vertical position $z^*(t)$ with respect to $\delta_v(t)$, i.e. $z^*(t) = z/\delta_v(t)$, and hence z^* is the rescaled distance from the plate in unit of BL thickness. The mean velocity profile $u^*(z^*)$ in this time-dependent frame is then calculated by averaging all values of $u(z, t)$ that were measured at different discrete time t but at the same relative position z^* , i.e. $u^*(z^*) = \langle u(z, t) | z = z^*\delta_v(t) \rangle$. The results are shown in Fig. 5(a), normalized by the maximum value of each profile $[u^*(z^*)]_{max}$. One sees excellent collapse of all profiles for the regions inside and around the viscous BL ($z^* \lesssim 2$), suggesting a universal BL profile for all Ra measured in the two cells. For comparison, we also calculate the time-averaged velocity $u(z) (= \langle u(z, t) \rangle)$ for each fixed position z . We note that $u^*(z^*)$ is more universal than $u(z)$ in the sense that profiles for different values of Ra collapse better in the time-dependent frame than they do in the laboratory frame.

To characterize the shape of the $u^*(z^*)$ profile more quantitatively, we examine its shape factor δ_d/δ_m , where $\delta_d = \int_0^\infty \{1 - \frac{u^*(z^*)}{[u^*(z^*)]_{max}}\} dz^*$ is the displacement thickness and $\delta_m = \int_0^\infty \{1 - \frac{u^*(z^*)}{[u^*(z^*)]_{max}}\} \{\frac{u^*(z^*)}{[u^*(z^*)]_{max}}\} dz^*$ is the momentum thickness [1]. Because of the zero mean-flow in the central region of a closed convection cell [12], $u^*(z)$ decays after reaching its maximum value and hence the above integrations are evaluated only over the range from $z^* = 0$ to where $u^*(z^*) = [u^*(z^*)]_{max}$. For comparison, we also show the shape factors of the $u(z)$ profiles measured in the laboratory frame, which are represented by the triangles in the inset of Fig. 5(a). It is seen that for all values of Ra, δ_d/δ_m of $u(z)$ are clearly smaller than 2.59 — the value of a Blasius laminar BL profile — but are larger than the value of 1.4 for a turbulent boundary layer. This is a quantitative indication that the present BL is neither fully turbulent nor strictly laminar, which is similar to the findings in [9]. On the other hand, the shape factors of $u^*(z^*)$ (red circles), measured in the time-dependent frame, are much closer to the Blasius value. In fact, for data measured in the large cell, δ_d/δ_m seems to have been perfectly

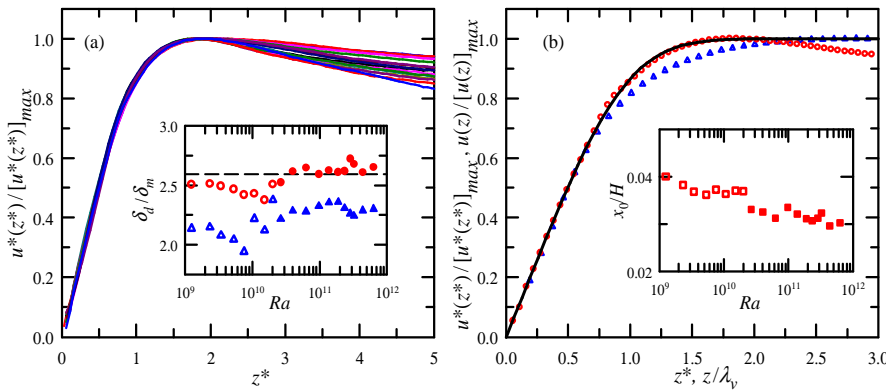


FIG. 5: (color online) (a) Normalized profiles of $u^*(z^*)$ for all measured Ra ranging from 1.25×10^9 to 6.4×10^{11} . Inset: the shape factors δ_d/δ_m of $u^*(z^*)$ (red circles) and $u(z)$ (blue triangles) vs. Ra , the dashed line represents the value of 2.59 for the Blasius BL. (b) Comparison among several velocity profiles: $u^*(z^*)$ (red circles), $u(z)$ (blue triangles), and the Blasius profile (black line). The data were measured at $Ra = 1.9 \times 10^{11}$. Inset: x_0/H vs. Ra . In both insets the solid (open) symbols are data from the large (small) cell.

“corrected” to the theoretical value. This implies that the velocity profiles obtained in the frame of $\delta_v(t)$ are of Blasius type. To see this more clearly, we directly compare in Fig. 5(b) the velocity profiles $u^*(z^*)$ and $u(z)$, measured in the time-dependent and laboratory frames respectively, with the theoretical Blasius profile. In the figure, $u^*(z^*)$ (circles) and $u(z)$ (triangles) are based on the same data set ($Ra = 1.9 \times 10^{11}$) and the Blasius profile (solid line) is obtained by numerically solving the two-dimensional boundary layer equations [1]. Here, to make a proper comparison, the initial slope of the Blasius profile is matched to that of the measured profiles by adjusting the path length x_0 in the similarity parameter $\eta = z\sqrt{u_{max}/2x_0\nu}$ [9]. An excellent coincidence between $u^*(z^*)$ and the Blasius profile is seen for $z^* \lesssim 2$. Whereas the values of $u(z)$ are clearly lower than those of the Blasius profile in the region around the viscous BL ($0.7 \lesssim z/\lambda_v \lesssim 2$), which may be attributed to the intermittent emissions of thermal plumes and is similar to previous findings [9]. If this can be generalized to other types of flows, it then suggests that the laminar Blasius profile can be restored even in the presence of intermittent eruption of coherent structures, like thermal plumes, if one measures the profile in the time-dependent reference frame that fluctuates with the instantaneous BL thickness $\delta_v(t)$. For $z^* \gtrsim 2$ the $u^*(z^*)$ profile deviates gradually from the Blasius profile because $u^*(z^*)$ decreases in the bulk region of the closed convection system. The fitting path length x_0 is plotted in the inset of Fig. 5(b). The values of x_0/H are much smaller than

the value of 0.5 assumed in the model of Grossmann and Lohse [14], but are consistent with the results of Ref. [9]. It is further found that x_0/H decreases slightly with increasing Ra , which may be a result of the path-length evolution of the large-scale circulation [15].

Finally, we check the scaling properties of $\delta_v(t)$. We use δ_v^{mp} as the typical viscous BL thickness. The best power-law fits give $\delta_v^{mp}/H \sim 4.5Ra^{-0.27 \pm 0.02}$ and $\delta_v^{mp}/H \sim 0.64Re^{-0.49 \pm 0.02}$ for the small cell and $\delta_v^{mp}/H \sim 2.5Ra^{-0.25 \pm 0.02}$ and $\delta_v^{mp}/H \sim 0.60Re^{-0.51 \pm 0.02}$ for the large cell, where $Re = [u^*(z^*)]_{max}H/\nu$ is the large-scale Reynolds number. All these results are in line with those obtained using the time-averaged profiles measured in the laboratory frame [10] and the measured δ_v^{mp}/H - Re scaling exponents are in good agreement with the theoretical value of -0.5 for the Blasius BL, further confirming the conclusion of the Blasius-type laminar BL in RB system [10, 14].

To summarize, we have developed a method to represent measured BL quantities in a time-dependent frame that fluctuates with the BL thickness such that the classical Blasius BL theory developed for laminar shear layers can now be applied to flows with strong fluctuations and intermittently eruptions of coherent structures.

We thank Chao Sun for providing us the PIV data measured in the small cell. This work was supported by the Research Grants Council of Hong Kong SAR (Nos. CUHK403806 and 403807). Q. Z. thanks supports of Shanghai NSF (No. 09ZR1411200) and Shanghai EDF (No. 09CG41).

-
- [1] H. Schlichting and K. Gersten, *Boundary Layer Theory*. (Springer, 8th ed., 2004).
 [2] A. Belmonte, A. Tilgner, and A. Libchaber, Phys. Rev. Lett. **70**, 4067 (1993); Phys. Rev. E **50**, 269 (1994).
 [3] Y.-B. Xin, K.-Q. Xia, and P. Tong, Phys. Rev. Lett. **77**, 1266 (1996); Y.-B. Xin and K.-Q. Xia, Phys. Rev. E **56**, 3010 (1997).
 [4] A. Naert, T. Segawa, and M. Sano, Phys. Rev. E **56**, R1302 (1997).
 [5] X.-L. Qiu and K.-Q. Xia, Phys. Rev. E **58**, 486 (1998);

- Phys. Rev. E **58**, 5816 (1998).
 [6] R. L. J. Fernandes and R. J. Adrian, Expl. Thermal Fluid Sci. **26**, 355 (2002).
 [7] S. Lam *et al.*, Phys. Rev. E **65**, 066306 (2002).
 [8] R. Verzicco and R. Camussi, J. Fluid Mech. **477**, 19 (2003).
 [9] R. du Puits, C. Resagk, and A. Thess, Phys. Rev. Lett. **99**, 234504 (2007).
 [10] C. Sun, Y.-H. Cheung, and K.-Q. Xia, J. Fluid Mech. **605**, 79 (2008); Q. Zhou and K.-Q. Xia, to be published.

- [11] G. Ahlers, S. Grossmann, and D. Lohse, *Rev. Mod. Phys.* **81**, 503 (2009).
- [12] K.-Q. Xia, C. Sun, and S.-Q. Zhou, *Phys. Rev. E* **68**, 066303 (2003).
- [13] W. S. Cleveland and S. J. Devlin, *J. Amer. Statist. Assoc.* **83**, 596 (1988).
- [14] S. Grossmann and D. Lohse, *J. Fluid Mech.* **407**, 27 (2000); *Phys. Rev. Lett.* **86**, 3316 (2001); *Phys. Rev. E* **66**, 016305 (2002); *Phys. Fluids* **16**, 4462 (2004).
- [15] J. J. Niemela and K. R. Sreenivasan, *Europhy. Lett.* **62**, 829 (2003); C. Sun and K.-Q. Xia, *Phys. Rev. E* **72**, 067302 (2005).